Room temperature electrodeposition of photoactive Cd(OH)$_2$ nanowires

M. Santamaria, P. Bocchetta *, F. Di Quarto

Dipartimento di Ingegneria Chimica dei Processi e dei Materiali, Università di Palermo, Viale delle Scienze, 90128 Palermo, Italy

ARTICLE INFO

ABSTRACT

Cd(OH)$_2$ nanowires (NWs) were successfully prepared by room temperature electrogeneration of base using Cd(NO$_3$)$_2$ aqueous electrolyte and Anodic Alumina Membrane (AAM) as template. Cd(OH)$_2$ films have been also deposited on tin-doped indium oxide (ITO) for comparison. SEM analysis shows high quality deposits made of closely packed nanowires (NWs) into AAM and uniform flake-like surface on ITO. XRD analysis reveals that Cd(OH)$_2$ films on ITO are polycrystalline, while the nanowires grow along the preferential directions [100] and [110]. Photoelectrochemical measurements show that Cd(OH)$_2$ NWs are photoactive materials with indirect and direct band gap of 2.15 and 2.75 eV, respectively.

© 2008 Published by Elsevier B.V.

1. Introduction

Nanostructured materials have attracted great interest due to their unique chemical and physical properties, which can be influenced not only by the preparation procedure but also by their shape and size [1,2]. The morphology of the nanostructures plays a key role especially on the optoelectronic properties of the materials, which determine the performances of semiconductors to be used in solar cells, as photo transistors and diodes, transparent electrodes, and so on. Cadmium hydroxide, Cd(OH)$_2$, is a wide band gap (>2 eV) semiconductor which can be used in numerous applications due to its optical and electrical properties as well as owing to the possibility to easily convert Cd(OH)$_2$ into CdO or into other functional materials (such as CdS or CdSe) [3,4]. Among the techniques successfully employed for the fabrication of Cd(OH)$_2$ nanostructures, the solvothermal synthesis [5] appears the only process able to produce high aspect ratio nanowires, with the disadvantages of using high temperature and long process times.

Recently, template-assisted electrochemical synthesis has been shown to be a versatile, simple and low temperature approach for the preparation of metals oxide/hydroxide nanostructures [6–10]. The deposition usually occurs through a mechanism of electroprecipitation, according to which base is generated at the cathode/electrolyte interface, where the hydroxide reaches its solubility product owing to the local increase of pH [11,12].

In the case of Cd, the reduction of Cd^{2+} ions to metallic Cd has a standard equilibrium potential higher with respect to the other metals whose hydroxides have been precipitated into AAMs

[7,9,10]. Thus, the reduction process involving Cd^{2+} can completely suppress the OH$^-$ generation from H$_2$O reduction, as reported in Ref. [13], where the cathodic polarization of AAM/Au in CdCl$_2$ aqueous electrolyte lead to the formation of Cd metallic nanowires. Moreover, the cathodic reaction can be substituted with O$_2$ reduction not involving water and CdO nanowires can be directly produced via AAM template in a totally anhydrous solvent (DMSO) at 80 °C [14]. The possibility to use this electrochemical route for the deposition of metal hydroxides M(OH)$_z$ is strictly related to the nobility of the metal ions due to the competition between the reduction of M^{z+} and the reduction of the species involved in the OH$^-$ production. For this reason, the choice of the electrolyte composition is crucial in determining the composition of the deposit.

In this work we have successfully deposited Cd(OH)$_2$ NWs into pores of AAM template via cathodic electrosynthesis from aqueous solution containing Cd(NO$_3$)$_2$ at room temperature. The idea is to induce the generation of OH$^-$ ions through the reduction of nitrate ions, which are more noble than Cd^{2+}. Cd(OH)$_2$ films have been also deposited on ITO substrate for comparison. Crystallinity and nature of the deposited films and nanostructures have been investigated through X-Ray Diffractometry, while the morphology has been observed by Scanning Electron Microscopy (SEM). Photoelectrochemical measurements have been carried out to estimate the band gap value of Cd(OH)$_2$ nanowires.

2. Experimental

The electrodeposition process was carried out in aqueous 0.05 M Cd(NO$_3$)$_2$ solution, by applying a constant cathodic current density of 1 mA cm^{-2} with a multichannel potentiostat VMP2 (Princeton

* Corresponding author. Tel.: +39 091 6567233; fax: +39 06 233211963.
E-mail address: bocchetta@dicpm.unipa.it (P. Bocchetta).

Applied Research). Commercial AAM (Anodisc-60 Whatman, average pore diameter 200 nm, porosity 43%) have been employed as template. Gold was sputtered on one side of AAMs in order to create conductive layer (Ar, 3 min, 30 mA). The AAM was supported in a holder with an exposed area of 2.54 cm². A classic three-electrode cell was employed with the AAM/Au as working electrode, a DSA (Dimensionally Stable Anode) electrode as counter electrode and a silver/silver chloride (Ag/AgCl) as reference electrode. Morphology and quality of the NWs have been investigated by using a Philips XL30 ESEM Scanning Electron Microscope. The AAM/NWs have been sometimes chemically etched in 1 M NaOH for 24 h in order to remove the AAM and filtered. X-ray Diffraction (XRD) analysis of

composite AAM/NWs arrays was realized by a Philips X-Ray Generator (Model PW 1130) and a PW (Model 1050) goniometry. The identification was performed according to the ICDD (The International Centre for Diffraction Data®) available cards. The experimental set-up for the photoelectrochemical investigations is described elsewhere [15]: a 450 W UV–VIS xenon lamp coupled with a monochromator (Kratos) allows monochromatic irradiation of the specimen surface through the electrochemical cell quartz windows. A two-phase lock-in amplifier (EG&G) was used in connection with a mechanical chopper (frequency: 13 Hz) in order to separate the photocurrent from the total current circulating in the cell due to the potentiostatic control. Photocurrent spectra reported below
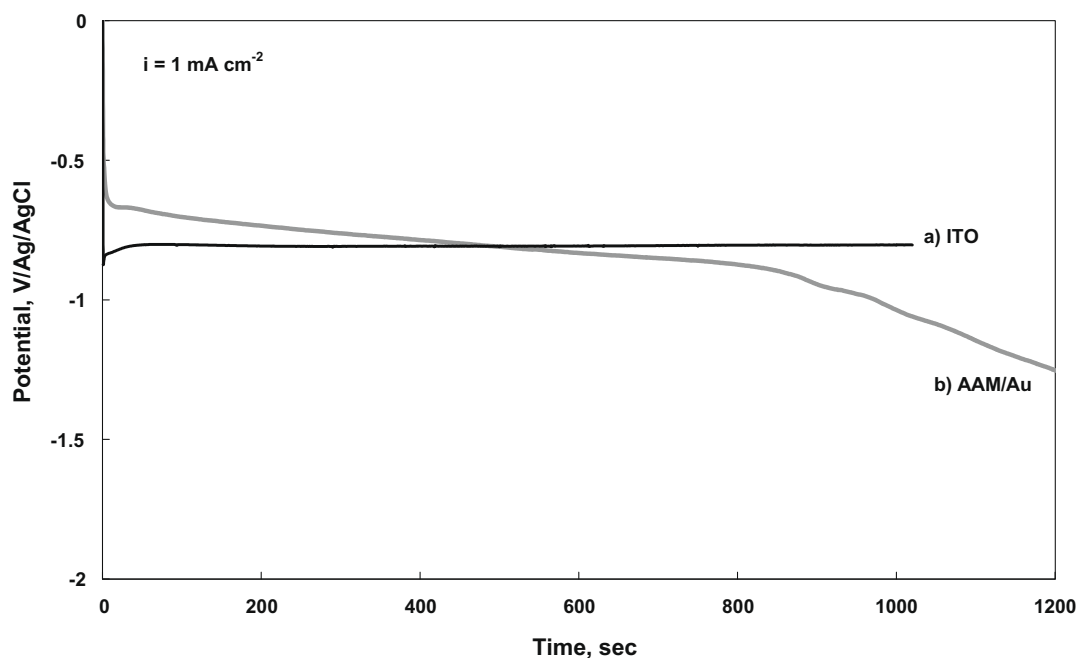

Fig. 1. Potential vs. time at 1 mA cm⁻² of Cd(OH)₂ from 0.05 M Cd(NO₃)₂ 6 H₂O aqueous solution at 25 °C. Substrate: (a) ITO; (b) AAM/Au.
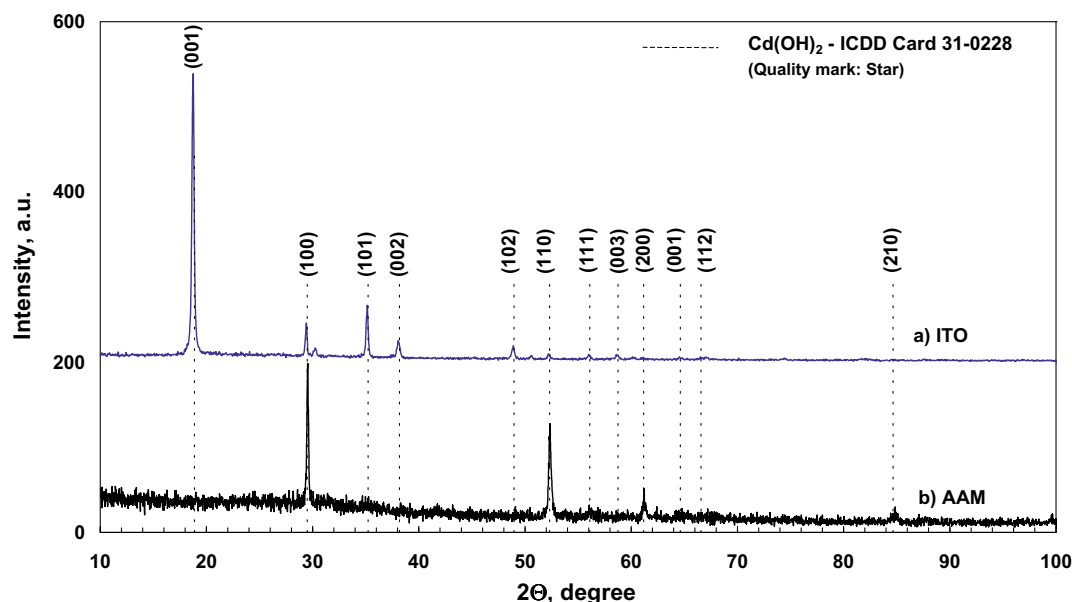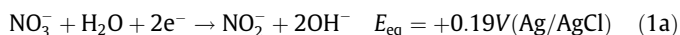

Fig. 2. XRD patterns of Cd(OH)₂ electrodeposited as described in Fig. 1 on (a) ITO for 20 min and into (b) AAM for 60 min.

are normalized for the photon flux of the light source at 400 nm (2.5×10^{15} photons s^{-1}). AAM has been partially dissolved in 0.1 M NaOH for 30 min before the measurement. All the experiments were performed in air at room temperature.

3. Results and discussion

In Fig. 1 the potential-time curves relating to AAM/Au and ITO working electrodes at 1 mA/cm^2 in 0.05 M Cd(NO$_3$)$_2$ (pH 5) are reported. The possible cathodic processes that can sustain the circulating current at the measured potentials are NO$_3^-$ and Cd^{2+} reduction. The equilibrium potentials (E_{eq}) for the corresponding half-cell reactions at pH 5 are:

$$NO_3^- + H_2O + 2e^- \rightarrow NO_2^- + 2OH^- \quad E_{eq} = +0.19 V(Ag/AgCl) \quad (1a)$$

$$Cd^{2+} + 2e^- \rightarrow Cd \quad E_{eq} = -0.64 \text{ V (Ag/AgCl)} \quad (1b)$$

In spite thermodynamically possible, the reduction of Cd^{2+} is excluded on the basis of XRD results (see below). Thus, the production of OH$^-$ ions according to Eq. (1a) is the main process with the subsequent precipitation of Cd(OH)$_2$.

In Fig. 2 XRD patterns of deposits obtained on ITO substrate and into AAMs template are compared. All the peaks can be attributed to pure Cd(OH)$_2$ hexagonal phase (ICDD Card # 31-0228). The XRD spectrum of Cd(OH)$_2$ on ITO shows peaks position and relative intensity basically consistent with the card, indicating that the deposit is typically polycrystalline. The XRD spectrum of Cd(OH)$_2$ NWs into AAM reveals two strong peaks at 2θ = 29.45 and 52.35°, whereas the peak [0 0 1] (relative intensity of 100%) is absent. This finding suggests a preferential electrochemical growth of the Cd(OH)$_2$ wires along the [1 0 0] and [1 1 0] crystallographic axes, in contrast to the random orientation for Cd(OH)$_2$ NWs prepared by hydrothermal synthesis [3].

Typical SEM images of Cd(OH)$_2$ NWs after removal of the template membrane are reported in Fig. 3a–c at different
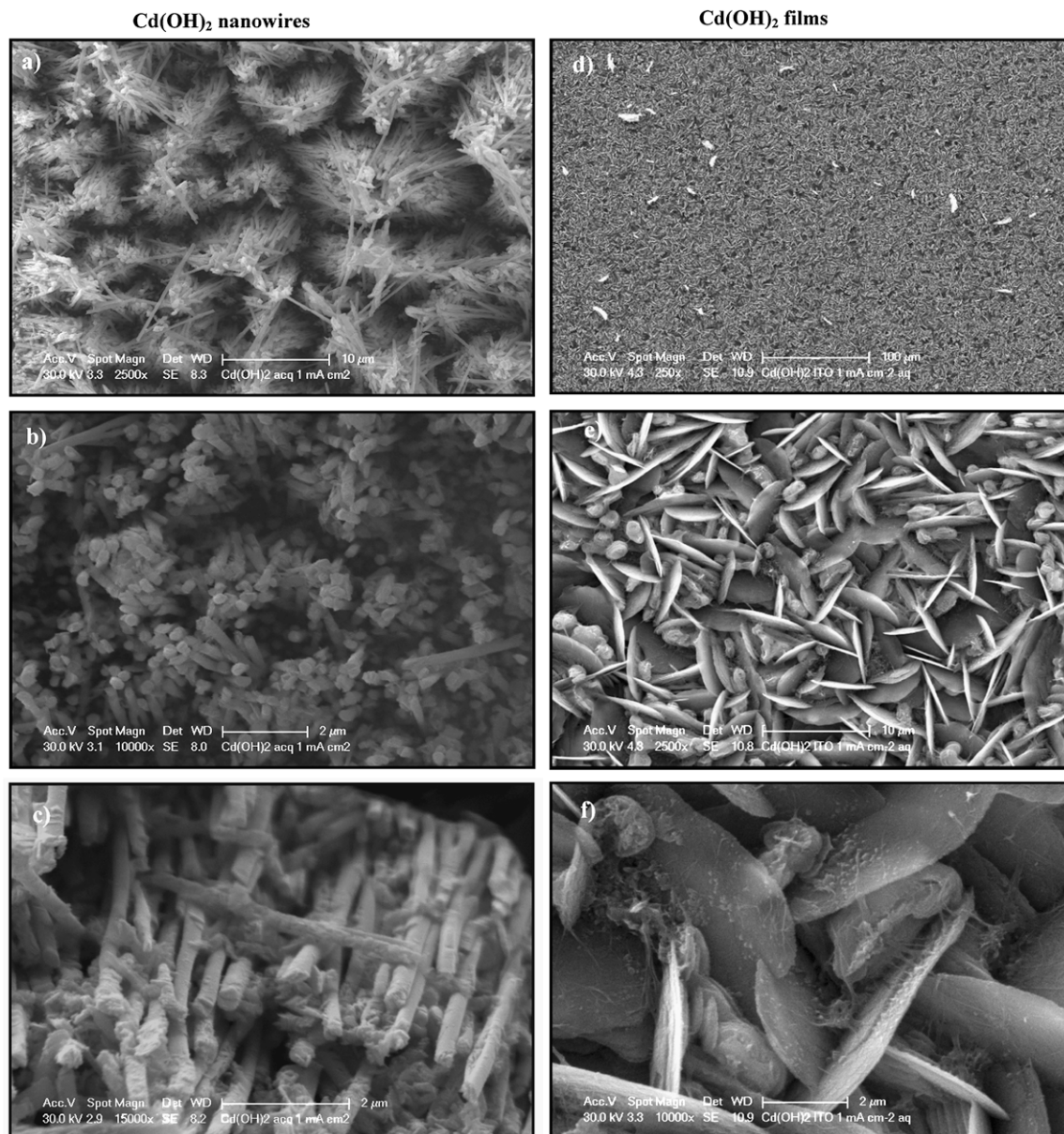

Fig. 3. SEM images of Cd(OH)$_2$ prepared as described in Fig. 1. (a–c) nanowires after AAM dissolution; (d–f) film on ITO.

magnifications. The analysis of several samples reveals that very well packed $Cd(OH)_2$ NWs are synthesized in a large scale. SEM surface images of $Cd(OH)_2$ films on ITO (Fig. 3d–f) points that the film is composed of well aggregated flakes uniformly distributed over the total electrodic area ($3 \, cm^2$).

In Fig. 4a we report the photocurrent spectrum relating to the $AAM/Cd(OH)_2$ NWs recorded by polarizing the electrode at -0.05 V (Ag/AgCl) in 0.1 M NaOH (pH 12.3). Manually chopped experiments at this potential revealed the presence of steady state cathodic photocurrent.

According to the Pourbaix diagram relating to Cd–H_2O system at room temperature, in these conditions Cd(II) is thermodynamically stable as $Cd(OH)_2$. The optical band gap of cadmium hydroxide NWs can be estimated according to the following equation valid for photon energies in the vicinity of the band gap:

$$(I_{ph}h\nu) \propto \left(h\nu - E_g^{opt}\right)^n \tag{2}$$

in which I_{ph}, the photocurrent yield, is proportional to the light absorption coefficient, $h\nu$ is the photon energy and the exponent n depends on the kind of optical transitions occurring under irradiation [15]. As shown in Figs. 4b and c, an indirect ($n = 2$) band gap of 2.1 eV and a direct ($n = 0.5$) band gap of ~ 2.7 eV can be estimated from the recorded photocurrent spectrum.

In Refs. [15,16] a correlation between the band gap of hydroxides and the square of electronegativity difference between the metal, χ_M, and hydroxyl group, χ_{OH}, has been proposed. In the previous work, the formation of hydroxides was supported by thermodynamic arguments or by indirect experimental evidence and, for a limited number of d metal hydroxides, the following best fitting equation has been obtained:

$$E_g = 0.65(\chi_M - \chi_{OH})^2 + 1.38 \ (eV) \tag{3}$$

where $\chi_{OH} = 2.85$ has been obtained as the arithmetic average between the value of hydrogen ($\chi_H = 2.2$) and that of oxygen ($\chi_O = 3.5$). By taking into account that the electronegativity of Cd is 1.7 in the Pauling scale, a band gap value of 2.24 eV can be estimated for $Cd(OH)_2$ according to Eq. (3), which exceeds the experimental one by ~ 0.14 eV. As suggested for $Co(OH)_2$ [17], this difference can be explained by taking into account that Eq. (3) has been derived for thin hydroxides films probably having an amorphous structure, whilst in the experimental conditions employed in this work, the formation of crystalline $Cd(OH)_2$ NWs and/or films has been proved.

By taking into account that the value of 2.75 eV has been reported for $Cd(OH)_2$ quantum dots chains [18], where an appreciable blue shift in value can be expected owing to the quantum confinement effects, we suggest that the optical fundamental gap of $Cd(OH)_2$ NWs is really indirect and quite near to the expected value (see Eq. (3)).

In summary, we have shown that high quality films and well-aligned compact nanowires of pure $Cd(OH)_2$ can be successfully synthesized by simple, inexpensive, and room temperature cathodic electrodeposition from Cd^{2+} containing aqueous solution introducing NO_3^- as strong oxidizing agent. $Cd(OH)_2$ NWs are photoactive with band gap value in agreement to that expected on the base of a previously proposed correlation between E_g and the electronegativity difference of metal and OH group [15–16].
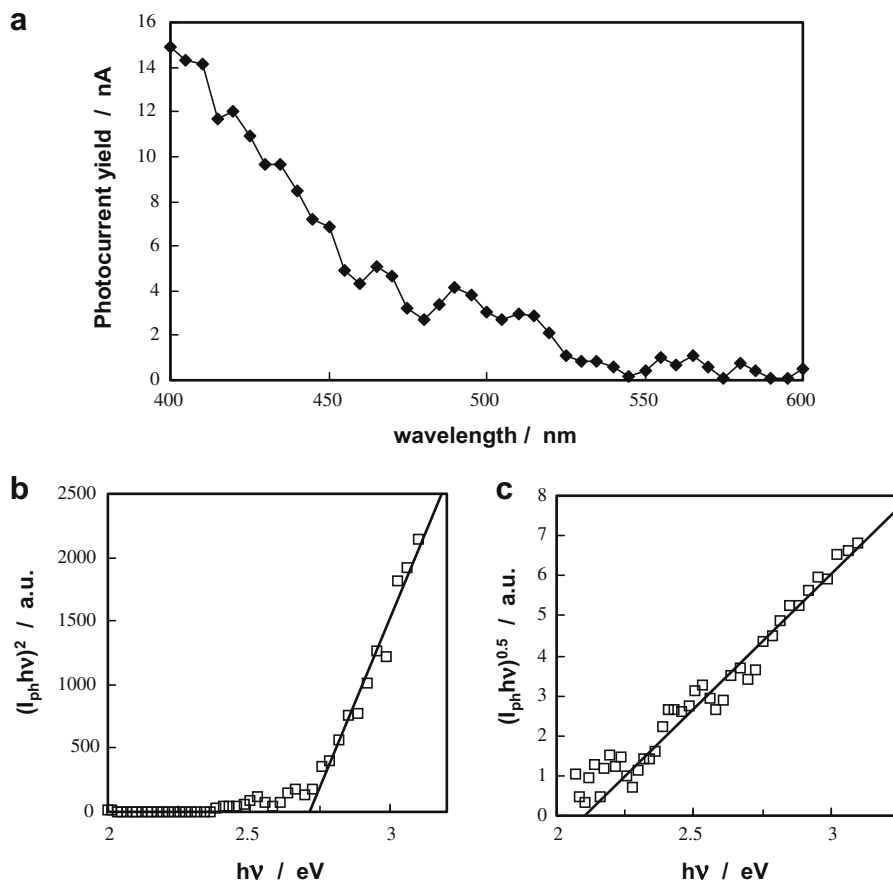
Fig. 4. (a) Photocurrent spectrum relating to $AAM/Cd(OH)_2$ NWs (prepared as described in Fig. 1) recorded at -0.05 V (Ag/AgCl) in 0.1 M NaOH. Band gap estimate assuming (b) direct and (c) indirect optical transitions.

Acknowledgments

References

[1] A.P. Alivisatos, Science 271 (1996) 933.
[2] C.M. Lieber, Solis State Commun. 107 (1998) 607.
[3] M. Ye, H. Zhong, W. Zheng, R. Liu, Y. Li, Langmuir 23 (2007) 9064.
[4] H.Z. Zhong, Y.C. Li, Y. Zhou, C.H. Yang, Y.F. Li, Nanotechnology 17 (2006) 772.
[5] B. Tang, L. Zhuo, J. Ge, J. Niu, Z. Shi, Inorg. Chem. 44 (2005) 2568.
[6] A. Daltin, A. Addad, J.-P. Chopart, J. Cryst. Growth 282 (2005) 414.
[7] P. Bocchetta, M. Santamaria, F. Di Quarto, Electrochem. Commun. 9 (2007) 683.
[8] K.-H. Wu, S.-Y. Lu, Electrochem. Solid-State Lett. 8 (2005) D9.
[9] P. Bocchetta, M. Santamaria, F. Di Quarto, Electrochem. Solid-State Lett. 11 (2008) K27.
[10] P. Bocchetta, M. Santamaria, F. Di Quarto, Electrochem. Solid-State Lett. 9 (2008) K97.
[11] G. Helen, A. Therese, P.V. Kamath, Chem. Mater. 11 (1999) 3561.
[12] M. Nobial, O. Devos, O.R. Mattos, B. Tribollet, J. Electroanal. Chem. 600 (2007) 87.
[13] Y.W. Wang, C.H. Liang, G.Z. Wang, T. Gao, S.X. Wang, J.C. Fan, L.D. Zhang, J. Mater. Sci. Lett. 20 (2001) 1687.
[14] Q. Wang, G. Wang, X. Wang, Int. J. Nanotechnol. 4 (2007) 110.
[15] F. Di Quarto, S. Piazza, M. Santamaria, C. Sunseri, in: H.S. Nalwa (Ed.), Handbook of Thin Film Materials, vol. 2, Academic Press, S. Diego, 2002, p. 373. Chapter 8.
[16] (a) F. Di Quarto, C. Sunseri, S. Piazza, M.C. Romano, J. Phys. Chem. B 101 (1997) 2519;
(b) F. Di Quarto, M.C. Romano, M. Santamaria, S. Piazza, C. Sunseri, Russ. J. Electrochem. 36 (2000) 1203;
(c) F. Di Quarto, M. Santamaria, C. Sunseri, Photoelectrochemical techniques in corrosion studies, in: P. Marcus, F. Mansfeld (Eds.), Analytical Methods in Corrosion Science and Technology, Taylor and Francis, Boca Raton, 2006, p. 697. Chapter 18.
[17] M. Santamaria, E. Adragna, F. Di Quarto, Electrochem. Solid-State Lett. 8 (2005) B12.
[18] R.S. Mane, S.-H. Han, Electrochem. Commun. 7 (2005) 205.